

We are IntechOpen, the world's leading publisher of Open Access books Built by scientists, for scientists

4,800

Open access books available

122,000

International authors and editors

135M

Downloads

Our authors are among the

154

Countries delivered to

TOP 1%

most cited scientists

12.2%

Contributors from top 500 universities



WEB OF SCIENCE™

Selection of our books indexed in the Book Citation Index
in Web of Science™ Core Collection (BKCI)

Interested in publishing with us?
Contact book.department@intechopen.com

Numbers displayed above are based on latest data collected.

For more information visit www.intechopen.com



Radiolabeled Nanoparticles for Molecular Imaging

Enrique Morales-Avila^{1,2}, Guillermina Ferro-Flores¹,
Blanca E. Ocampo-García^{1,2} and Flor de María Ramírez¹

¹*Instituto Nacional de Investigaciones Nucleares,*

²*Universidad Autónoma del Estado de México,
Mexico*

1. Introduction

Molecular imaging (MI) comprises non-invasive monitoring of functional and spatiotemporal processes at molecular and cellular levels in humans and other living systems. In contrast to conventional diagnostic imaging, MI seeks to probe the molecular abnormalities that are the basis of disease rather than capture the images of the end effects of the molecular alterations. Imaging techniques such as magnetic resonance imaging (MRI), single photon emission computed tomography (SPECT), positron emission tomography (PET) and optical fluorescence imaging (OI) have been used to monitor such processes. Radionuclide-based imaging methods, such as SPECT and PET, use internal radiation that is administered through a target-specific molecule labeled with a radionuclide at doses free of pharmacologic side effects. Nuclear imaging is an established clinical MI modality that, compared to other modalities, offers better sensitivity and has no tissue penetration limits (Massoud & Gamghir, 2003; Ferro-Flores et al., 2010a). Nuclear technologies have been evolving toward greater sensitivity due to enhanced hardware development, such as multi-pinhole acquisitions methods or pixelated semiconductor detectors. In parallel with the hardware advances, steady progress is being made in image-processing algorithms, and such algorithms may soon provide substantial reduction in SPECT acquisition times without sacrificing diagnostic quality (Madsen, 2007). The fusion of nuclear and anatomical images from computed tomography (CT) into a single imaging device (SPECT/CT and PET/CT) has been very useful for clinical oncology (Hong et al., 2009a).

According to the American Society for Testing and Materials (ASTM), the term nanoparticles describes a sub-classification of ultra-fine solids with dimensions from 1 nm to 100 nm and novel properties that distinguish them from the bulk material (ASTM, 2006). Nanoparticles produce multivalent effects due to multiple simultaneous interactions between the biomolecules conjugated to the nanoparticle surface and specific receptors for those biomolecules on the cell surface (Montet et al., 2006). Nanoparticles can be near infrared (NIR)-fluorescent (e.g. nanocrystals or quantum dots) or can have magnetic properties (e.g. iron oxide nanoparticles).

Therefore, the first aim during the development of radiolabeled nanoparticles is to maximize the binding affinity via multimeric receptor-specific biomolecules based on the

multivalency principle. Large numbers of antibodies, peptides or any molecule with biological activity can be linked to the surface of a single radiolabeled nanocrystal (quantum dot), metal nanoparticle (iron oxide and gold) or single-walled carbon nanotube (SWNT) to improve imaging of tumors over-expressing those specific antigens or receptors.

In general, different imaging techniques are complementary rather than competitive. Consequently, the second aim of engineering radiolabeled nanoparticles is to develop dual-labeled imaging agents that target the same ligand. This allows for cross validation between nuclear and fluorescence optical images, MRI and nuclear images, or trimodal nuclear-MRI-fluorescence images.

The third aim is related to therapeutic properties. Gold nanoparticles and SWNT, which are designed to absorb in the NIR spectrum, cause irreversible thermal cellular destruction when they are irradiated using a laser (NIR light). It is important to remember that “the magic bullet does not exist” when it comes to cancer therapy; therefore, increasing the therapeutic response requires the application of combined modalities with multiple therapeutic agents. For example, gold nanoparticles or SWNT radiolabeled with beta-particle emitters could represent a unique, multifunctional and target-specific pharmaceutical that could be administered as a single drug. This pharmaceutical would be capable of functioning, simultaneously, as both a targeted radiotherapy system and a photothermal therapy system.

This chapter covers recent major advancements in design, synthesis, physicochemical characterization and molecular recognition assessment of radiolabeled synthetic nanoparticles for molecular imaging and highlights the therapeutic possibilities of these nanosystems.

2. General aspects of radiolabeled nanoparticles

Multivalent interactions regulate a wide variety of cellular processes, such as cell surface recognition events that involve inflammation and tumor metastasis. Multivalency is a design principle by which organized arrays amplify the strength of a binding process, e.g. the binding of multimeric peptides to specific receptors on a cell surface (Ocampo-Garcia et al., 2011a).

Nanoparticles can be design as multimeric systems to produce multivalent effects. The physical and chemical properties of nanoparticles play an important role in determining particle-cell interactions, cellular trafficking mechanisms, biodistribution, pharmacokinetics and optical properties. Important nanoparticle properties include chemical composition of the core, size, shape, surface charge and surface chemistry.

The synthesis of nanoparticles with a variety of physicochemical properties has led to important advances. Among these, gold nanoparticles are of particular importance to SPECT/CT or PET/CT molecular imaging due to the relative ease of surface modification and radiolabeling, their biocompatibility, resistance to oxidation and extraordinary optical properties (Giljohann et al., 2010).

Nanoparticles of semiconductors are densely packed inorganic fluorescent semiconductor crystals with excellent optical properties, and these can be radiolabeled for PET/NIR imaging (Erathodiyil & Ying, 2011).

Radiolabeled iron oxide nanoparticles have been designed for use in SPECT/MRI and PET/MRI dual techniques (Torres et al., 2011; Jarret et al., 2008). Other radiolabeled nanosystems have also been proposed for biomedical applications, and these include single wall carbon nanotubes (Hong et al., 2009b), fullerenes (Qingnuan et al., 2002), multiwall carbon nanotubes (Guo et al., 2007) and CuS nanoparticles (Zhou et al., 2010).

Radiolabeled nanoparticles conjugated to target specific molecules can be directly used as agents for diagnosis. The most common radionuclides for SPECT imaging include ^{99m}Tc ($t_{1/2}=6\text{ h}$) and ^{111}In ($t_{1/2}=2.8\text{ days}$), and the most common for PET are ^{64}Cu ($t_{1/2}=12.7\text{ h}$), ^{18}F ($t_{1/2}=109.8\text{ min}$) and ^{68}Ga ($t_{1/2}=68.1\text{ min}$). Moreover, radiolabeling is used to study the biokinetics of new devices based on nanoparticles that comprise radiopharmaceuticals, drug/gene delivery systems or plasmonic photothermal therapy enhancers. Many types of radiolabeled nanoparticles have three main components: the core, the targeting biomolecule and the radiotracer group (Fig. 1). The targeting biomolecule includes a component with high affinity for target epitopes; radiolabeling can be performed with or without slight modifications of the original nanoparticle (NP) surface. For ligands to bind effectively, each radionuclide can be conjugated directly on the NP surface, with or without a spacer, or can be attached to the NP during chemical synthesis. The spacer groups between the NP surface and the radionuclide or the biomolecule can be a simple hydrocarbon chain, a peptide sequence or a poly-ethyleneglycol linker.

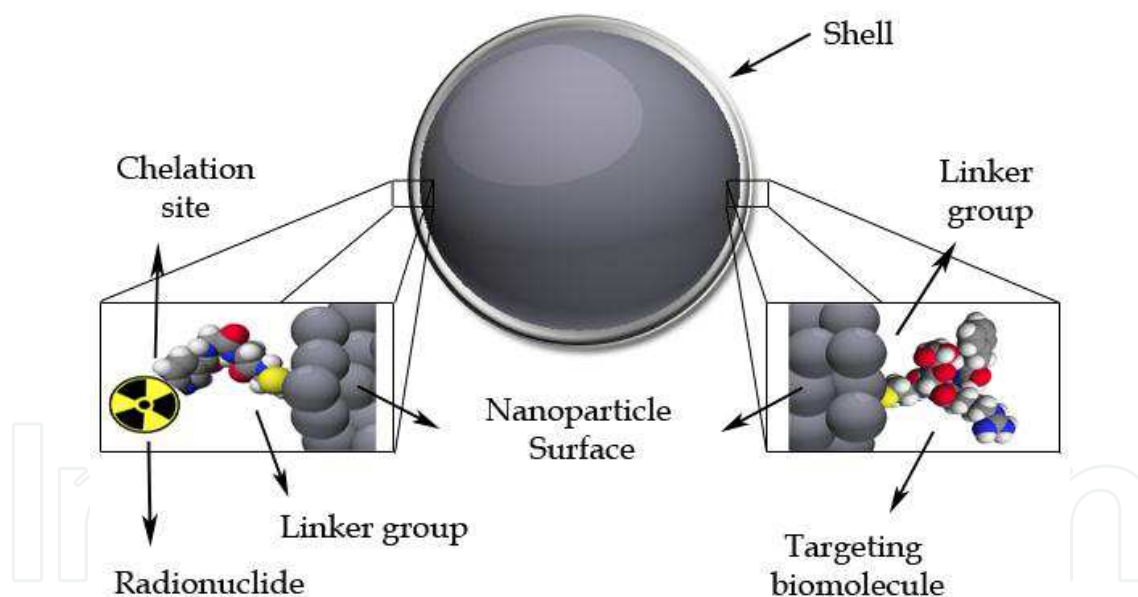


Fig. 1. Schematic structure of a radiolabeled nanoparticle design for molecular imaging

3. Radiolabeled nanoparticles for SPECT molecular imaging

Peptide receptors are proteins that are overexpressed in numerous human cancer cells. These receptors have been used as molecular targets, allowing radiolabeled peptides to identify tumors. The gastrin-releasing peptide receptor (GRP-r) is overexpressed in prostate and breast cancer, and ^{99m}Tc -Lys³-bombesin has been reported as a radiopharmaceutical with specific binding to cells expressing GRP-r (Ferro-Flores et al., 2006; Santos-Cuevas et al., 2008). Integrin $\alpha_V\beta_3$ plays a critical role in tumor angiogenesis, and radiolabeled cyclic-Arg-Gly-Asp

(RGD) peptides have been used for noninvasive imaging of tumor $\alpha_v\beta_3$ expression (Liu, 2008, 2009). Mannosylated macromolecules labeled with ^{99m}Tc have displayed properties suitable for use in sentinel lymph node detection; these radiopharmaceuticals are considered target-specific because they exhibit specific binding to mannose receptors that are expressed on lymph node macrophages (Vera et al., 2001; Takagi et al., 2004).

Based on the observations above, ^{99m}Tc -labeled gold nanoparticles conjugated to Lys³-bombesin, RGD peptides or thiol-mannose have been prepared as multimeric systems showing properties suitable for use as target-specific agents for molecular imaging of GRP receptor-positive tumors, tumor $\alpha_v\beta_3$ expression and sentinel lymph node detection, respectively. ^{99m}Tc - and ^{111}In -labeled carbon nanotubes, ^{125}I -labeled silver nanoparticles and ^{99m}Tc -labeled iron oxide nanoparticles have also been reported for SPECT imaging (Table 1). The strategies of synthesis and functionalization for these nanoparticles are discussed in the following sections.

3.1 Synthesis of NP cores

The most common nanomaterials reported for SPECT imaging are iron oxide NPs, gold NPs, silver NPs and carbon nanotubes. NPs usually have optical or magnetic properties that can be used for molecular imaging, whereas polymer- or liposome-based NPs do not produce imaging signals by themselves.

NP core synthesis generally follows standardized strategies; for example, the most popular method of synthesis for gold nanoparticles (AuNPs) is based on the use of HAuCl_4 (Au III) salt, which is reduced to metallic Au(0) in aqueous solution and stabilized with a chemical agent. The classical sodium citrate reduction is the oldest and most widely used method (Daniel & Astruc, 2004), but there are different techniques to produce AuNPs with different sizes and shapes using reduction agents stronger than citrate (such as NaBH_4), different organic solvents and/or different stabilizer surfactants. Most of the stabilizer surfactants are quaternary ammonium salts, such as cetyltrimethylammonium bromide (CTAB), didodecyldimethylammonium bromide (DDAB) and tetradodecylammonium bromide (TTAB). Anionic surfactant syntheses have also been reported (Zhang et al., 2006). Anisometric gold colloids (rods) can be prepared by adding gold nuclei to HAuCl_4 growth solutions (formed by reduction of HAuCl_4 with phosphorus), and the growth of the gold nanorods is initiated with the addition of H_2O_2 (Huang et al., 2009). Electrochemical and photochemical reduction, microwave, ultrasound and laser ablation have also been used for AuNP synthesis (Ferro-Flores et al., 2010b; Huang et al., 2009). The Au(0) core is essentially inert and non-toxic (Connor et al., 2005). AuNPs exhibit narrow and intense absorption and scattering bands due to the phenomenon of plasmon resonance. This occurs at the resonance condition of the collective oscillation that the conduction electrons experience in an electromagnetic field of the appropriate wavelength. The plasmon resonance band for ordinary 20 nm gold nanospheres is at 520 nm, in the middle of the visible spectrum, but this can be red-shifted into the NIR spectrum. Rod-shaped NPs exhibit two plasmon resonance bands due to oscillation of the conduction electrons along the short axis and the long axis of the particles. The former plasmon band is called the transverse resonance and the latter the longitudinal resonance. While the transverse plasmon band occurs in the neighborhood of 520 nm, the longitudinal band is red-shifted between 675–850 nm in the interest of optical imaging. This occupies the most important part of the “optical imaging window” where light penetration in tissue is high due to reduced scattering and absorption

coefficients. Optical imaging techniques that rely on scattering and/or absorption contrast to detect pathological tissue could benefit from the use of gold nanoparticles with targeting capability (Huang et al., 2009).

Core	Surface molecule/ Target	Radionuclide and Chelator	Application (Reference)
Gold nanoparticles	RGD/ $\alpha_v\beta_3$ integrin	^{99m}Tc -HYNIC	SPECT/CT imaging of $\alpha_v\beta_3$ integrin expression, and multimodal probe for possible thermotherapy (Morales-Avila et al., 2011)
	Lys ³ -Bombesin/ Gastrin releasing peptide receptors		SPECT/CT imaging of gastrin releasing peptide-receptor in breast and prostate cancer detection, and multimodal probe for possible thermotherapy (Mendoza-Sanchez et al., 2010)
	Mannose/ Mannose receptors		SPECT/CT imaging for mannose receptors in sentinel lymph node detection in breast cancer, and multimodal probe for possible thermotherapy (Ocampo-Garcia et al., 2011a, 2011b)
	--	^{99m}Tc -DTPA	PEG-coated AuNPs for drug delivery vehicles and diagnostic imaging agents (Zhang et al., 2009)
Carbon nanotubes	--	^{99m}Tc -C ₆₀ (OH) _x ^{111}In -DTPA	SPECT/CT image and platform for delivery of biologic, radiologic and chemical cargo to target tissues. (Qingnuan et al., 2002; Guo et al., 2007; Chan et al., 2004; Singh et al., 2006; McDevitt et al., 2007)
	Rituximab (anti-CD20)/ CD20 epitope on human non Hodgkin lymphoma cells	^{111}In -DOTA	
Silver nanoparticles	Poly (N-vinyl-2-pyrrolidone)	^{125}I	<i>In vivo</i> imaging and biodistribution of radiolabeled NPs (Chrastina & Schnitzer, 2010)
Supermagnetic Iron oxide, SPIO	Alendronate/ osteoclastic surface	^{99m}Tc -DTPA	Platform for SPECT/MRI images (Torres et al., 2011)

Table 1. Radiolabeled nanoparticles for SPECT imaging

Iron oxide NPs can be synthesized via the coprecipitation of Fe^{2+} and Fe^{3+} aqueous salt solutions, which results in the addition of a base. The size, shape and composition of NPs depend on a number of factors, including: the type of salts used (e.g., chlorides, sulfates, nitrates or perchlorates), the Fe^{2+} and Fe^{3+} ratio, pH and ionic strength of the media. A variety of other methods, based on the principle of precipitation in highly constrained domains, have been developed and these include sol-gel preparation, polymer matrix-mediated synthesis and precipitation using microemulsions and vesicles (Kogan et al., 2007).

Silver nanoparticles can be synthesized in large quantities by reducing silver nitrate with ethylene glycol in the presence of poly(vinyl pyrrolidone) (PVP). The presence of PVP and its molar ratio relative to silver nitrate is important in determining the geometric shape and size of the product. The size, shape, and structure of metal nanoparticles are important because there is a strong correlation between these parameters and optical, electrical, and catalytic AgNP properties (Sun & Xia, 2002).

Carbon nanotubes (CNT) are essentially hexagonal networks of carbon atoms arranged like a layer of graphite rolled into a cylinder consisting of pure carbon units, the C_{60} fullerene. Methods such as electric arc discharge, laser vaporization and chemical vapor deposition techniques are well known to produce a wide variety of single- (SWNT) and multi-walled (MWNT) CNTs. Catalytic chemical vapor deposition is the most commonly used, whereas the water-assisted synthesis method for NTs produces highly organized intrinsic nanotube structures. The water-stimulated synthesis enhances catalytic activity resulting in massive growth of super-dense and vertically aligned nanotubes (Hata et al., 2004). SWNTs produce high optical absorbance in the NIR (Kam et al., 2005). It has been well documented that water-solubilized nanotubes with high hydrophilicity are non-toxic, even at high concentrations (Dumortier et al., 2006).

3.2 Preparation of radiolabeled NP-conjugates

To achieve recognition of the molecular target, specific biomolecules are used as ligands and these are conjugated to the AuNP surface. These ligands include sugars, antibodies, nucleic acids, proteins and peptides. All of these biomolecules must offer low nonspecific binding, high affinity to their binding sites, no immunogenicity, fast accumulation at the target, fast blood clearance, and preferably exhibit no peripheral metabolic activity or toxicity. The biomolecules are frequently attached to the surface of the nanoparticle via electrostatic interactions; however, a covalent bond is preferred to prevent release of the attached biomolecules *in vivo*. The chemical bond occurs between the AuNP surface and the peptide containing sulfhydryl (-SH) groups (usually from cysteine) with high affinity toward the gold atoms. The -SH group forms a 'staple motif' chemical model comprised of two thiol groups interacting with three gold atoms in a bridge conformation (Jadzinsky et al., 2009).

Two main strategies for binding peptides to AuNPs are commonly used. The first is the direct conjugation of the peptide by means of a terminal thiol (cysteine) or an *N*-terminal primary amine (Levy et al., 2004; Porta et al., 2007), and the second is an indirect conjugation with a linker that contains both a thiol group (that binds the nanoparticle) and a carbonyl terminal group, that is activated and conjugated to biological active peptides using the carbodiimide-coupling chemistry (Wang et al., 2005; Cheung et al., 2009). An advantage of the direct conjugation strategy is that it does not require the use of linkers with long chains

as spacers between the NP and the conjugated peptides. This is important because the introduction of spacers and an increase in linker length has been proven to significantly alter the peptide-multivalency effect, which may correlate to a decrease in the effective peptide molarity (Kubas et al., 2010).

Current methodologies for SPECT molecular imaging require an additional ligand that is appended to the AuNP surface, and this ligand functions as a chelator of the radiometal. Two different kinds of molecules can be bound to the AuNP surface to produce hybrid radiolabeled AuNP-peptide systems. In our research, we have reported two different radionuclide chelators to generate radiolabeled gold nanoparticles. Mendoza-Sanchez et al., (2010), Ocampo-Garcia et al., (2011b) and Morales-Avila et al., (2011) demonstrated radiolabeling of AuNPs using 6-hydrazinopyridine-3-carboxylic(HYNIC)-GGC peptide. With this approach, HYNIC was added as a ^{99m}Tc chelator group, -Gly-Gly- as a spacer group and -Cys as the active group that interacted with the nanoparticle surface (Fig. 2). In the second approach, the HYNIC-Tyr³-Octreotide (HYNIC-TOC) was used for AuNP radiolabeling, whereby the HYNIC group was the ^{99m}Tc chelator and the cysteine contained in the disulphide bridge or the ϵ -amine of lysine was the reactive group for AuNP conjugation (Ocampo-Garcia et al., 2011a) (Fig. 3).

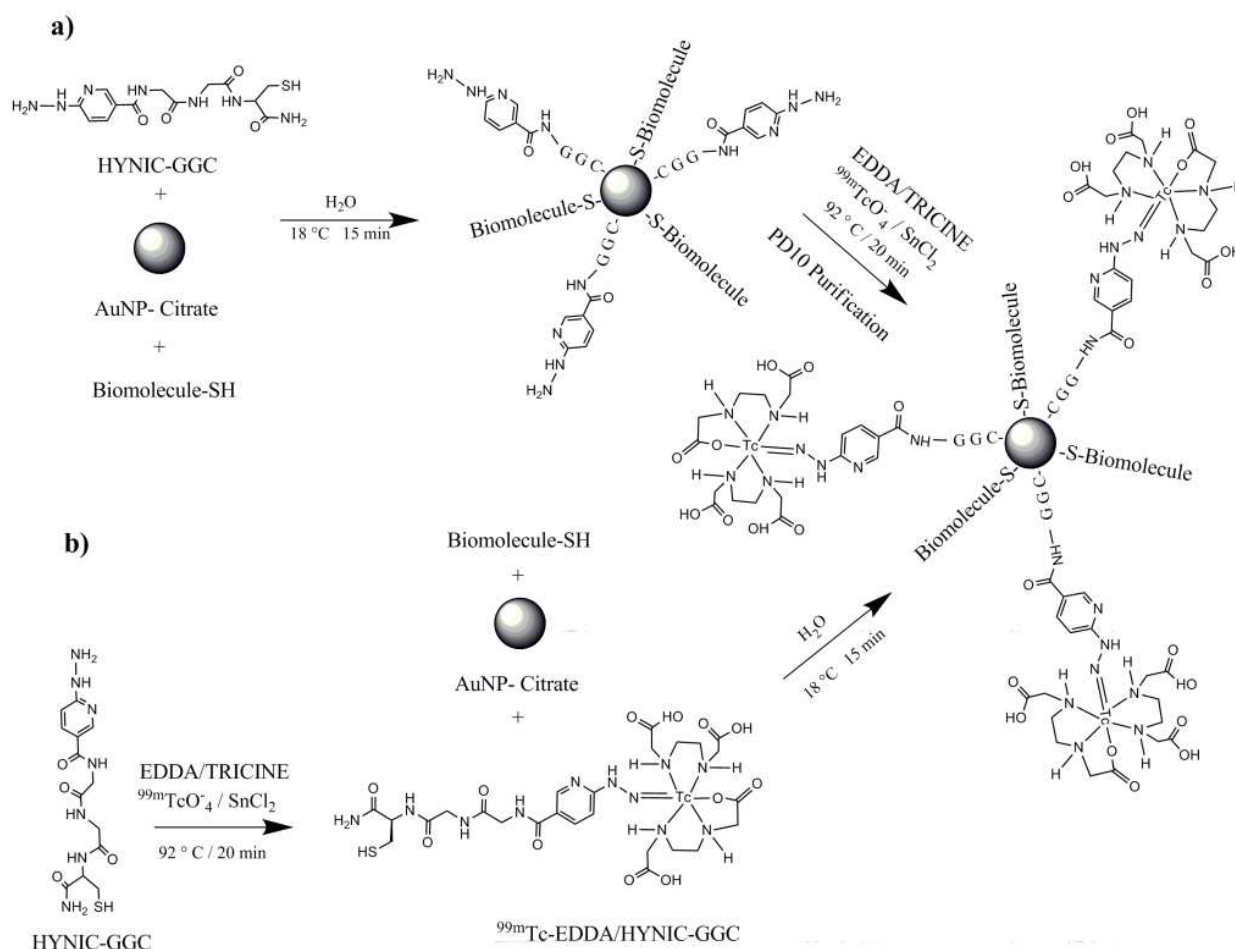


Fig. 2. Radiolabeling of gold nanoparticles conjugated to biomolecules using HYNIC-GGG as ^{99m}Tc chelator: a) radiolabeling after biomolecule conjugation to AuNP and b) conjugation and radiolabeling in a single step without further purification.

Mendoza-Sanchez et al., (2010) and Ocampo-Garcia et al., (2011b) conjugated peptides to the gold nanoparticle surface using a posterior radiolabeling process. This process was conducted by adding ethylenediaminediacetic acid (EDDA)/Tricine, SnCl_2 (as reducing agent) and $^{99\text{m}}\text{Tc}$ -pertechnetate to 1 mL of HYNIC-GGC-AuNP followed by incubation at 100°C for 20 min. The mixture was purified by size-exclusion chromatography (PD-10 column, Sephadex G-25) using injectable grade water as the eluent by collecting 0.5 mL fractions. The first peak (3.0–4.0 mL) corresponded to the void volume of the column and contained $^{99\text{m}}\text{Tc}$ -EDDA/HYNIC-GGC-AuNP (a radioactive red color solution), while the second peak corresponded to $^{99\text{m}}\text{Tc}$ -EDDA (6.0–8.0 mL). Free $^{99\text{m}}\text{TcO}_4^-$ and $^{99\text{m}}\text{Tc}$ -colloid remained in the PD-10 column (Fig. 2a). In a second approach (Morales-Avila et al., 2011), the peptide conjugation to AuNPs and the radiolabeling were carried out in a single step without further purification (Fig. 2b).

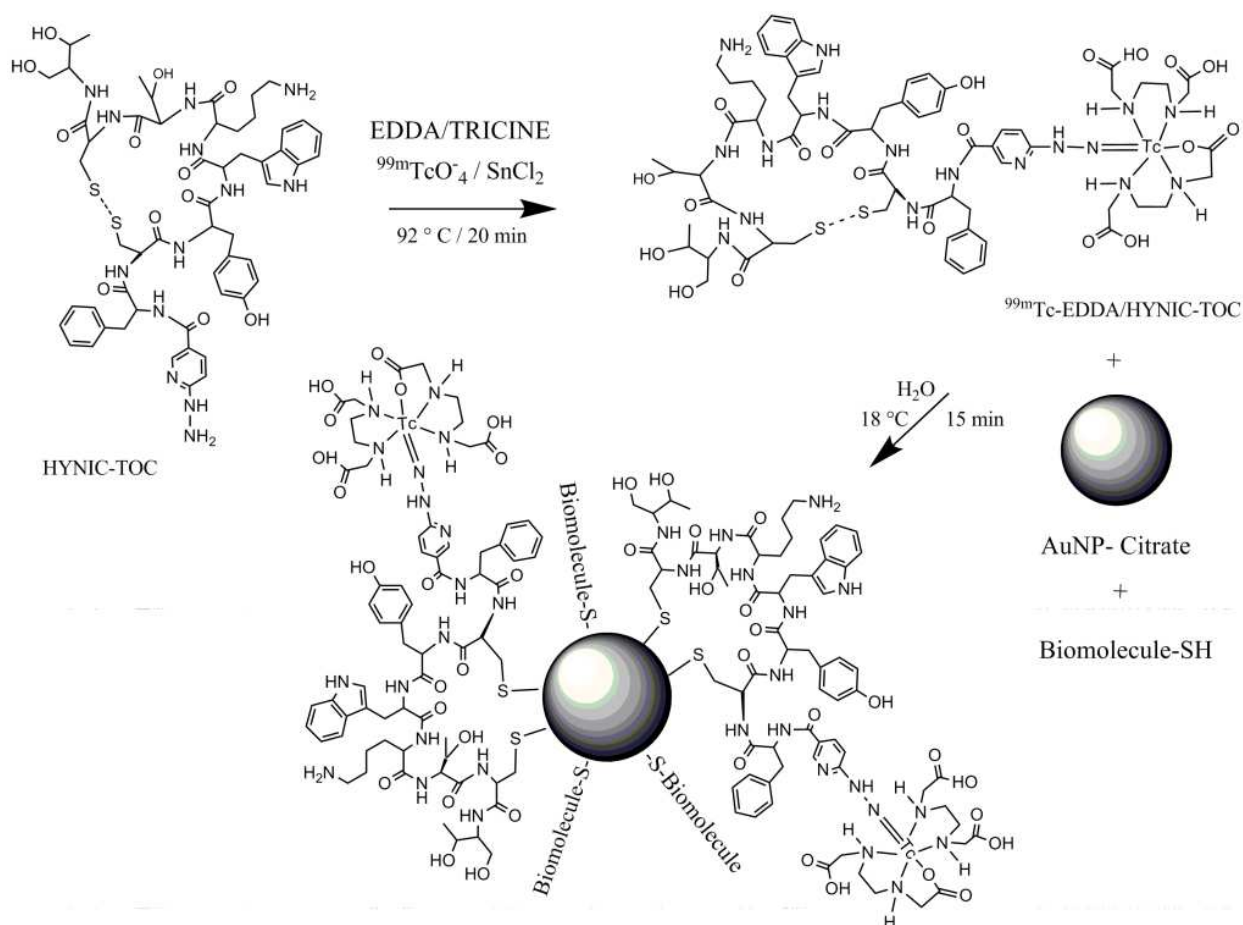


Fig. 3. Radiolabeling of gold nanoparticles conjugated to biomolecules using HYNIC-TOC as $^{99\text{m}}\text{Tc}$ chelator .

Zhang et al. (2009) obtained ^{111}In -labeled polyethylene-glycol (PEG)-AuNPs using diethylenetriaminepentaacetic acid-thioctic acid (DTPA-TA) as radiometal chelator. They found a strong dependency between pharmacokinetics/biodistribution and the size and density of PEG coating on the AuNP surface.

Chan et al. (2004) prepared carbon-encapsulated $^{99\text{m}}\text{Tc}$ nanoparticles. Fullerenes can be directly labeled with $^{99\text{m}}\text{Tc}$ using ascorbic acid/ SnCl_2 as reducing agents to form

$^{99m}\text{Tc-C}_{60}(\text{OH})_x$, however, biodistribution studies indicated that the radionanoparticles were distributed in all tissues (Qingnuan et al., 2002). The ^{99m}Tc -glucosamine-MWNT, also labeled by the direct method, is water-soluble, and further modification of this system may allow the development of a versatile delivery system for molecular targeting (Guo et al., 2007).

^{111}In -labeled carbon nanotubes were synthesized by Singh et al. (2006). The ammonium-functionalized CNTs (single- and multi-walled) were prepared following the 1,3-dipolar cycloaddition method to be covalently bound to DTPA. Biodistribution studies showed a rapid blood clearance (half-life=3 h) with renal excretion. Radiolabeling of CNTs with ^{111}In has also been reported by McDevitt et al., 2007. In general, CNTs are functionalized with 2-(4-isothiocyanatobenzyl)-1,4,7,10-tetraazacyclododecane-1,4,7,10-tetraacetic (DOTA-NCS) via thiolurea bonding and radiolabeled by adding ^{111}In chloride to the DOTA-CNT conjugate.

Chrastina & Schnitzer (2010) reported the synthesis of silver nanoparticles labeled with iodine-125 to track *in vivo* tissue targeting with SPECT images. Poly(N-vinyl-2-pyrrolidone)-capped silver nanoparticles (average size 12 nm) were labeled by chemisorptions, whereby chloramine-T (N-chlorobenzenesulfonamide) was immobilized on a polystyrene backbone. The radio-solution was removed and added to a dispersion of unfunctionalized Ag nanoparticles. Unbound iodide-125 was removed by size exclusion chromatography on Sephadex G-25 columns. Radiochemical yields higher than 95% were obtained. Radiolabeled AgNPs were characterized by UV-Vis spectrometry (410 nm).

Torres et al., (2011) reported the development of a new class of dual-modality imaging agents based on the conjugation of radiolabeled bisphosphonates (BP) directly to the surface of superparamagnetic iron oxide (SPIO) nanoparticles (5 nm, Fe_3O_4 core). The SPIO labeling with ^{99m}Tc -DTPA-alendronate was performed in a single step at room temperature. The radiolabeled nanoparticles showed excellent stability, making the conjugate suitable for SPECT-CT/MRI imaging.

3.3 Structural, chemical and radiochemical characterization

Several methods have been used for the structural characterization of nanoparticles, including X-ray diffraction (XRD), small-angle X-ray scattering (SAXS), microscopic techniques such as scanning electron microscopy (SEM), high-resolution transmission microscopy (HRTEM) and scanning probe microscopy (SPM). For the chemical characterization of the biomolecule-nanoparticle conjugate, spectroscopic methods have been applied to confirm the chemical interaction and functionalization of NPs with the biomolecules. These methods include UV-Vis, infrared, Raman, fluorescence and XPS spectroscopy. For example, in the case of peptides conjugated to AuNPs, the vibrational spectroscopic techniques can be used to confirm that the biomolecule displaces the carboxylate groups of the citrate on the AuNP surface. The structured spectra can be used to confirm that AuNPs were functionalized with peptides, because several well defined bands with vibrational frequencies in the region of those associated with the main functional groups of the peptides can be observed in the AuNP-peptide conjugate, even though these will have characteristics of the AuNP-peptide because the bands shift to lower or higher energies and increase in intensities (Suruypaul et al., 2008; Morales-Avila et al., 2011). Additionally, the Au-S bond shows a characteristic band at $279 \pm 1 \text{ cm}^{-1}$ identified by far-

infrared spectroscopy (Ocampo-Garcia et al., 2011a). In UV-Vis spectroscopy a red shift in the maximum absorbance of the AuNP is representative of the peptide conjugation process, while the small change in the surface plasmon resonance position occurs as the result of the peptide adsorption on the AuNP surface (Kogan et al., 2007; Ferro-Flores et al. 2010b). The orbital energies of Au-Au or AuNP (Au^0) and Au-S (Au^{+1}) bonds are related to changes in the oxidative states (Au^0 to Au^{+1}); therefore, in XPS analyses the shift of electron binding energies to higher values in the AuNP-peptide conjugates, with respect to AuNPs, is an intrinsic property of the interaction between gold core electrons and the peptide (Mendoza-Sanchez et al., 2010; Ocampo-Garcia et al., 2011b).

The methods frequently used to determine radiochemical purity and assess quality control of the radiolabelled nanoparticles include instant thin layer chromatography (ITLC), which has the advantage of being very quick and easy to use, and size-exclusion high performance liquid chromatography (SE-HPLC) that can be used as an accurate method depending on the NPs size. PD-10 columns and ultrafiltration can be used as easy purification methods and to determine radiochemical purity (Ocampo-Garcia et al., 2011a).

3.4 Biological recognition

It has been demonstrated that multimeric systems of $^{99\text{m}}\text{Tc}$ -AuNP-biomolecules exhibit properties that make them suitable for use as target-specific agents for molecular imaging of tumors and sentinel lymph node detection. For example, *in vitro* binding studies of $^{99\text{m}}\text{Tc}$ -AuNP-RGD conducted in $\alpha_V\beta_3$ receptor positive C6 glioma cancer cells showed specific recognition for those receptors (Morales-Avila et al., 2011). Moreover, $^{99\text{m}}\text{Tc}$ -AuNP-Lys³-bombesin showed specific recognitions for GRP receptors in PC3 cancer cells (Mendoza-Sanchez, et al., 2010) and $^{99\text{m}}\text{Tc}$ -AuNP-mannose demonstrated specificity for mannose receptors (Ocampo-Garcia et al., 2011a). Micro-SPECT/CT images of these radiopharmaceuticals have shown a clear tumor uptake or lymph node accumulation (Fig. 4).

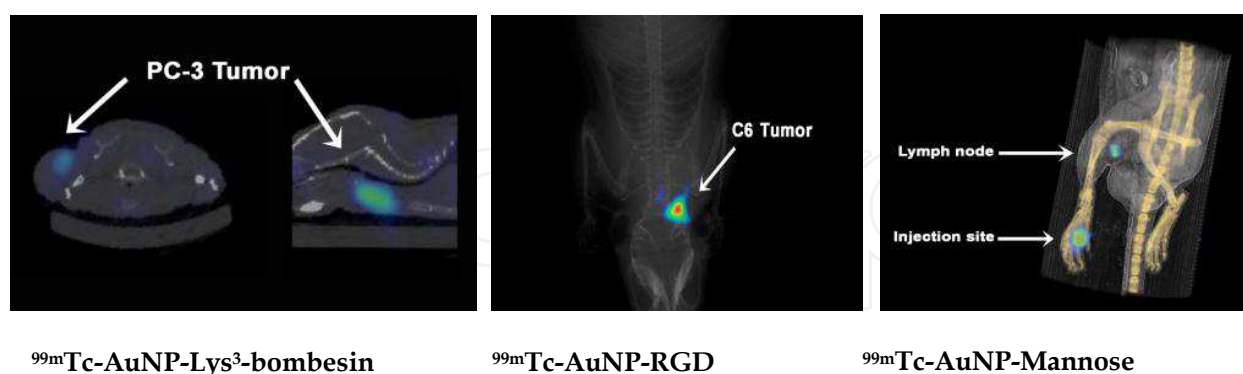


Fig. 4. Micro-SPECT/CT images of $^{99\text{m}}\text{Tc}$ -labeled gold nanoparticles in mice with induced tumors (conjugates of Lys³-bombesin and RGD) and in Wistar rat (mannose conjugate).

The ^{111}In -DTPA-TA-AuNP-PEG system has shown a prolonged blood circulation and significant tumor uptake by the enhanced permeability and retention effect, making of the radiolabeled AuNPs a promising drug delivery vehicle and diagnostic imaging agent (Zhang et al., 2009).

The multifunctional system of carbon nanotubes, conjugated to both anti-CD20 (Rituximab) and ^{111}In -DOTA-NCS, demonstrated ability of this double conjugate to specifically target tumor cells *in vitro* (in CD20+ specific Daudi cells) and tumors *in vivo* using a murine model of disseminated Lymphoma (McDevitt et al. 2007).

4. Radiolabeled nanoparticles for PET molecular imaging

PET is a nuclear imaging technique used to map biological and physiological processes in living subjects following the administration of radiolabeled probes. In PET, the radionuclide decays and the resulting positrons subsequently interact with nearby electrons after travelling a short distance (~ 1 mm) within the body. Each positron-electron transmutation produces two 511-keV gamma photons in opposite trajectories, and these two gamma photons may be detected by the detectors surrounding the subject to precisely locate the source of the decay event. Subsequently, the “coincidence events” data can be processed by computers to reconstruct the spatial distribution of the radiotracer (Chen & Conti, 2011). Several positron-emitting radionuclides have been used in the development of radiolabeled nanoparticles. These radionuclides include ^{64}Cu (E_{max} 657 keV), ^{18}F (E_{max} 635 keV) and ^{68}Ga (E_{max} 1.90 MeV), which are described in the following sections.

4.1 ^{64}Cu -labeled nanoparticles

The ^{64}Cu radionuclide can be effectively produced using both reactor- and accelerator-based methods. Its use as a positron emitter has grown, and it has been reported to be suitable for the radiolabeling of proteins, antibodies and peptides. In addition, ^{64}Cu has been investigated as a promising radiotracer for real-time PET monitoring of regional drug concentration and for pharmacokinetics applications. Its integration as a structural component of nanoparticles produces multimeric systems suitable for therapy and PET imaging (Zhou et al., 2010).

To date, nanocrystals (quantum dot), iron oxide nanoparticles, SWNT and gold nanoparticles (nanoshells) have been functionalized with ^{64}Cu ligands for PET/MRI or PET/NIR fluorescence imaging and therapy. In these multiple combinations, the same molecular target can be evaluated with two different imaging modalities. These groupings allow the strengths of each to improve the overall diagnostic accuracy, and this approach provides a synergistic effect, increasing expectations for high sensitive and high-resolution imaging (Hong, 2009).

Quantum dots (QDs) or nanocrystals are fluorescent semiconductor nanoparticles (2-10 nm) with many unique optical properties including bright fluorescence, resistance to photobleaching, and a narrow emission bandwidth (Ferro-Flores et al., 2010a). Their fluorescence emission wavelength can be continuously tuned from 400 nm to 2000 nm by changing both the particle size and chemical composition. Their quantum yields are as high as 85 %. The particles are generally made from hundreds to thousands of atoms (~ 200 -10,000 atoms) of IIB and VIA family elements (e.g. CdSe and CdTe) or IIIA and VA family elements (e.g. InP and InAs). Recent advances have allowed the precise control of particle size, shape and internal structure (core-shell, gradient alloy or homogenous alloy) (Yu et al., 2003). As cadmium is potentially toxic, Gao et al. (2004) developed a class of QD conjugates that contains an amphiphilic triblock copolymer for *in vivo* protection and multiple PEG

molecules for improving biocompatibility and circulation. InAs/InP/ZnSe Core/Shell/Shell quantum dots without Cd have significantly lower intrinsic toxicity compared to QDs containing elements such as cadmium (Xie et al., 2008).

A dual-modality PET/NIR fluorescent peptide has been recently reported (Cai et al., 2007; Chen et al., 2010). A QD (QD705; emission maximum, 705 nm) with an amine-functionalized surface was modified with RGD (90 peptides per QD) or the vascular endothelial growth factor (VEGF) and 1,4,7,10-tetraazacyclododecane-N,N',N'',N'''-tetraacetic acid (DOTA) chelator for integrin- $\alpha_v\beta_3$ or VEGF imaging. PET/NIR imaging, tissue homogenate fluorescence measurement, and immunofluorescence staining were performed with U87MG human glioblastoma tumor-bearing mice to quantify the ^{64}Cu -DOTA-QD-RGD and ^{64}Cu -DOTA-QD-VEGF uptake in tumor and major organs. Excellent linear correlation was obtained between the results measured by *in vivo* PET imaging and those measured by *ex vivo* NIR fluorescent imaging and tissue homogenate fluorescence. Histologic examination revealed that ^{64}Cu -DOTA-QD-RGD targets primarily the tumor vasculature through a RGD-integrin interaction, with little extravasation. The authors concluded that this dual-function probe has significantly reduced potential toxicity and overcomes the tissue penetration limitation of optical imaging, requisite for quantitative targeted imaging in deep tissue.

Iron oxide nanoparticles have magnetic properties and have been extensively investigated for biomedical applications due to their excellent biocompatibility and ease of synthesis. Jarrett et al. (2008) recently reported a dual-mode imaging probe for PET/MRI that was designed for vascular inflammation, and this probe was based on iron oxide nanoparticles coupled to ^{64}Cu . The labeling of SPIONs was made by coordination of ^{64}Cu to the chelating bifunctional ligand S-2-(4-isothiocyanatobenzyl)-1,4,7,10-tetraazacyclododecane-1,4,7,10-tetraacetic acid (*p*-SCNBz-DOTA) and followed by conjugation to the nanoparticle. For the dextran sulfate coated nanoparticles, the particle surface was modified to contain aldehyde groups that can be conjugated to the amine-reactive *p*-SCN-Bz-DOTA chelator. Xie et al. (2010) encapsulated iron oxide nanoparticles (IONPs) into human serum albumin (HSA) matrices. The HSA coated IONPs (HSA-IONPs) were dually labeled with ^{64}Cu -DOTA and Cy5.5, and tested in a subcutaneous U87MG xenograft mouse model. *In vivo* PET/NIR fluorescence/MRI tri-modality imaging showed massive accumulation in lesions, high extravasation rate, and low uptake of the particles by macrophages at the tumor area. Glaus et al. (2010) prepared ^{64}Cu -DOTA-PEG-SPIOs which demonstrated strong MR and PET signals and high stability in mouse serum for 24 h at 37 °C.

To image $\alpha_v\beta_3$ expression, multifunctional ^{64}Cu -labeled IONPs conjugated to RGD have been reported. Lee et al. (2008) developed the ^{64}Cu -DOTA-IO-RGD system (diameter: 45 ± 10 nm) containing 35 RGD peptide molecules and 30 DOTA chelating units per nanoparticle. The receptor-binding affinity studies for $\alpha_v\beta_3$ integrin in U87MG cells showed an IC₅₀ value of 34 ± 5 nM. cRGDfC and the macrocyclic 1,4,7-triazacyclononane-N,N',N''-triacetic-thiol derivative (NOTA-SH) were conjugated onto the iron oxide nanoparticles. ^{64}Cu -labeled SPIONs conjugated to cRGDfC demonstrated a good U87MG tumor-targeting capability and tumor contrast by PET/MRI dual-modality imaging (Yang et al., 2011).

Liu et al. (2007) investigated the biodistribution of ^{64}Cu -labeled SWNTs conjugated to polyethylene-glycol-DOTA and RGD in mice with U87MG-induced tumors using PET, *ex vivo* biodistribution and Raman spectroscopy. The results showed a high ^{64}Cu -DOTA-PEG-

SWNT-RGD tumor accumulation (~7% at 1 h) that was attributed to the multivalent effect of the SWNTs.

Gold nanoshells (NSs) are core/shell particles comprised of a gold shell and a dielectric silica core with peak plasmon resonances tunable to desired wavelengths by adjusting the relative core and shell thicknesses. At NIR wavelengths, light penetrates up to several centimeters in tissue. NSs absorb in the NIR wavelength and efficiently convert incident light to heat (eg, a 120-nm core diameter and a 14-nm-thick shell result in an absorption peak between 780 nm and 800 nm). Xie et al. (2011) reported the preparation of ^{64}Cu -DOTA labeled NSs conjugated to cRGDFK and evaluated the *in vivo* biodistribution and tumor specificity of these in live nude rats bearing head and neck squamous cell carcinoma (HNSCC) xenografts. The potential therapeutic properties were also evaluated by subablative thermal therapy of tumors. PET/CT imaging showed a high tumor uptake even at ~20 h postinjection and the thermal therapy study showed a high degree of tumor necrosis.

Core	Surface molecule/Target	^{64}Cu Chelator	Imaging Modality	Reference
Quantum Dots	RGD/ $\alpha_v\beta_3$ integrin or VEGF/VEGF-r	DOTA	PET/NIR fluorescence	Cai et al., 2007; Chen et al., 2010
Iron oxide nanoparticles	RGD/ $\alpha_v\beta_3$ integrin	DOTA and <i>p</i> -SCN-Bz-DOTA	PET/MRI	Lee et al., 2008; Jarret et al., 2008
		NOTA-SH		Yang et al., 2011
	PEGylated phospholipids	DOTA	PET/MRI	Glaus et al., 2010
	Human serum albumin and Cy5.5	DOTA	PET/MRI/NIR fluorescence	Xie et al., 2010
Carbon nanotubes	RGD/ $\alpha_v\beta_3$ integrin	PEG-DOTA	PET/NIR fluorescence	Liu et al., 2007
Gold nanoshells	RGD/ $\alpha_v\beta_3$ integrin	DOTA	PET/CT imaging and thermotherapy	Hie et al., 2011

Table 2. ^{64}Cu -labeled nanoparticles for PET imaging

4.2 ^{18}F labeled iron oxide nanoparticles for PET/MRI

The main requirement for MRI is the efficient capture of magnetic nanoparticles by the cell, and when a cell is sufficiently loaded with magnetic material, MRI can also be used for cell tracking. The synthesis and *in vivo* characterization of iron oxide nanoparticles labeled with ^{18}F was reported by Devaraj et al. (2009). This particle consists of cross-linked dextran

molecules held together in core-shell formation by a superparamagnetic iron oxide core and functionalized with the radionuclide ^{18}F in high yield, via “click” chemistry. Such nanoparticles could accurately detect lymph nodes (LNs), which are critical for assessing cancer metastasis. *In vivo* PET/MRI images could clearly identify small (~1 mm) LNs along with precise anatomical information.

4.3 ^{68}Ga labeled nanoparticles

Stelter et al. (2009) covalently bound the transfection agent HIV-1 Tat (peptide derived from the transcription protein transactivator of the human immunodeficiency virus), the fluorescent dye fluorescein isothiocyanate and ^{68}Ga to the aminosilane-coated superparamagnetic nanoparticle. PET imaging and MRI revealed increasing hepatic and splenic accumulation of the particles over 24 h in Wistar rats. Hepatogenic HuH7 cells were labeled with the radionanoparticles and injected them intravenously into rats, followed by animal PET and MRI imaging. *In vitro* studies in hepatogenic HuH7 cells showed a rapid intracellular accumulation of the labeled nanoparticles and without any signs of toxicity. *In vivo* dissemination of the labeled cells was followed by dynamic biodistribution studies. This radionanoconjugate can be applicable to efficient cell labeling and subsequent multimodal molecular imaging. Moreover, their multiple free amino groups suggest the possibility of further modifications and might provide interesting opportunities for various research fields.

A quadruple imaging modality made using nanoparticles that is capable of concurrent fluorescence, bioluminescence, bioluminescence resonance energy transfer (BRET), PET and MRI has been reported (Hwang et al., 2009). A cobalt-ferrite nanoparticle surrounded by rhodamine (MF) was conjugated with luciferase (MFB) and p-SCNbnNOTA (2-(4-isothiocyanatobenzyl)-1,4,7-triazacyclonane-1,4,7-triacetic acid) followed by $^{68}\text{GaCl}_3$ (magnetic-fluorescent-bioluminescent-radioisotopic particle, MFBR). Confocal microscopy revealed good transfection efficiency of MFB into cells and BRET was also observed in MFB. A good correlation among rhodamine, luciferase, and $^{68}\text{GaCl}_3$ was found in MFBR, and the activities of each imaging modality increased dose-dependently with the amount of MFBR in the C6 cells. *In vivo* optical images were acquired from the thighs of mice after intramuscular and subcutaneous injections of MFBR-laden cells. MicroPET and MR images showed intense radioactivity and ferromagnetic intensities with MFBR-laden cells. The multimodal imaging strategy could be used as a potential imaging tool to improve the diagnostic accuracy.

5. Radiolabeled nanoparticle for therapy

Radiolabeled nanoparticles represent novel agents with huge potential for clinical radiotherapy applications. McDevitt et al. (2010) proposed the radiolabeling of carbon nanotubes (DOTA-NTs, diameter of 1.4 nm.) functionalized by the anti-CD20 monoclonal antibody (Rituximab), the α -particle emitter ^{225}Ac and the β -particle emitter ^{90}Y . Alpha-emitters can be efficient therapeutics against small-volume tumors and micrometastatic cancers due to the linear energy transfer that is 500 times greater than that of β particles; hence, damaged cells have inadequate capability to repair DNA injury, and cell death may result. Beta-particle emitters are the most widely used radionuclides among the cancer

therapeutic agents because the localized decay in target cells generates DNA damaging free radicals, which can induce apoptosis (Fig. 4). Kucka et al. (2006) have also proposed the astatination of silver nanoparticles conjugated to poly(ethylene oxide) as possible carriers of the α -particle emitter ^{211}At .

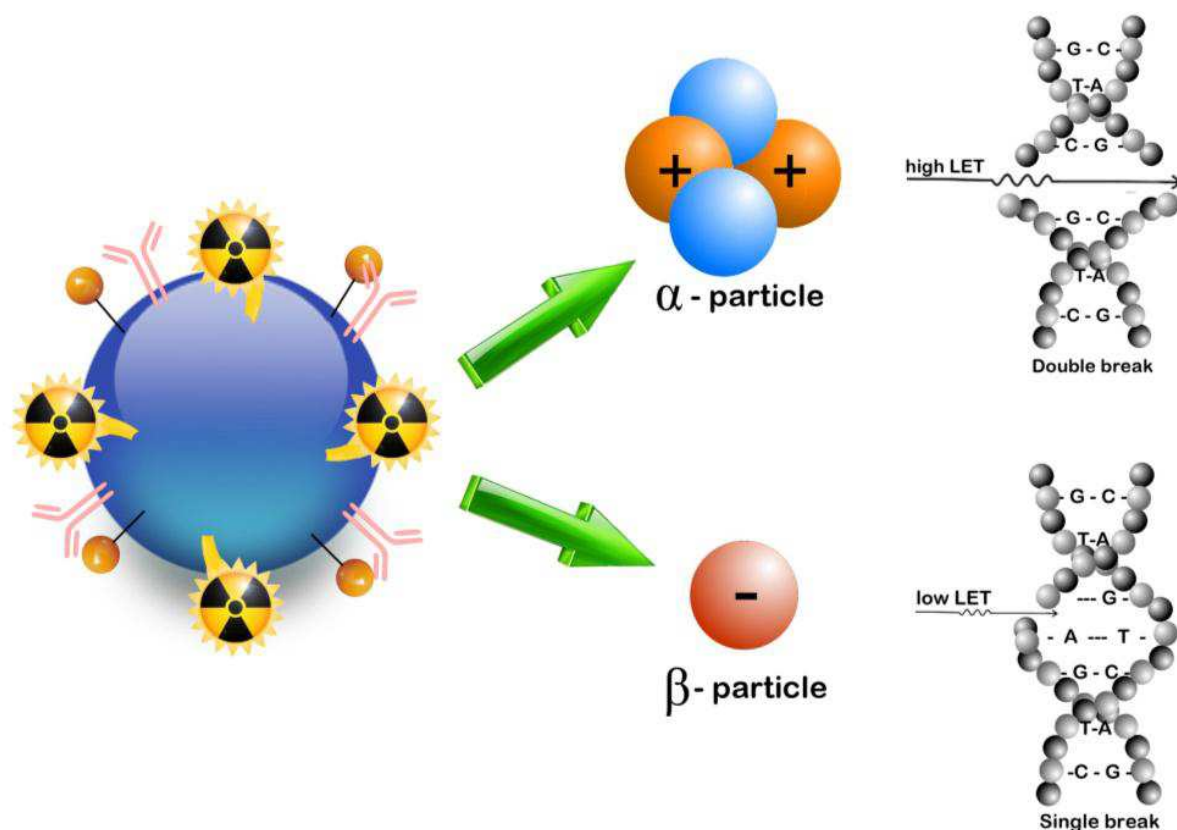


Fig. 4. Schematic representation of radiolabeled nanoparticles for therapeutic applications

The impermeable nature of the cell plasma membrane limits the therapeutic uses of many macromolecules. Several cell penetrating peptides, such as the HIV-1 Tat peptide, have been shown to traverse the cell membrane (where integral protein transduction domains (PTDs) are responsible for cellular uptake) and to reach the nucleus while retaining biological activity. PTDs can enable the cellular delivery of conjugated biomolecules and even nanoparticles, but nuclear delivery needs other strategies. Berry et al. (2007) developed biocompatible gold nanoparticles of differing sizes, functionalized with the HIV Tat-PTD, with the aim of producing nuclear targeting agents. The particles were subsequently tested *in vitro* on a human fibroblast cell line, and the results demonstrated successful nanoparticle transfer across the plasma membrane with 5 nm particles achieving nuclear entry while larger 30 nm particles were retained in the cytoplasm, suggesting entry was blocked via nuclear pores dimensions. $^{99\text{m}}\text{Tc}$ internalized in cancer cell nuclei acts as an effective system of targeted radiotherapy because of the Auger and internal conversion electron emissions near DNA. The HIV Tat(49-57) is a cell penetrating peptide that reaches DNA (Santos-Cuevas et al., 2011). Therefore, $^{99\text{m}}\text{Tc}$ -labeled gold nanoparticles (5nm) prepared by the methods previously described (Ocampo-Garcia et al., 2011b; Morales-Avila et al., 2011) and conjugated to the HIV Tat(49-57) peptide, could potentially be a multifunctional system with properties suitable for targeted radionuclide therapy.

The β -particle emitter ^{188}Re has been conjugated to NPs for radiotherapy purposes. In 2004, Cao et al. prepared silica-coated magnetite nanoparticles immobilized with histidine. ^{188}Re was linked on their surface by the complexation of $[\text{}^{188}\text{Re}(\text{CO})_3(\text{H}_2\text{O})_3]^+$ to the imidazolyl groups of histidine, obtaining a labeling yield of 91%. A direct labeling method has also been reported that radiolabels SPIONs with rhenium-188 (Liang et al., 2007). The radiolabeling efficiency was about 90%, with good *in vitro* stability. ^{188}Re labeled SPIONs demonstrated the ability to kill SMMC-7721 liver cancer cells.

Photothermal ablation (PTA) therapy is a minimally invasive alternative to conventional approaches for cancer treatment. NPs, primarily gold nanostructures such as gold nanoshells, nanorods, nanocages and hollow nanospheres but also carbon nanotubes, have been investigated as photothermal coupling agents to enhance the efficacy of PTA therapy. These plasmonic nanomaterials exhibit strong absorption in the NIR region (700-1100 nm) and offer the opportunity to convert optical energy into thermal energy, enabling the deposition of otherwise benign optical energy into tumors for thermal ablation of tumor cells, as recently demonstrated Xie et al. (2011). Furthermore, AuNPs can be labeled with α - or β -particle emitter radionuclides and linked to target specific biomolecules to produce both thermotherapy and radiotherapy effects on cancer cells.

Zhou et al. (2010) synthesized and evaluated a novel class of chelator-free $[\text{}^{64}\text{Cu}]\text{CuS}$ nanoparticles (NPs) suitable both for PET imaging and as photothermal coupling agents for photothermal ablation. $[\text{}^{64}\text{Cu}]\text{CuS}$ NPs possess excellent stability, and allow robust noninvasive micro-PET imaging. The CuS NPs display strong absorption in the near-infrared (NIR) region (peak at 930 nm); passive targeting prefers the tumor site, and mediated ablation of U87MG tumor cells occurs upon exposure to NIR light both *in vitro* and *in vivo* after either intratumoral or intravenous injection. The combination of small diameter (11 nm), strong NIR absorption, and integration of ^{64}Cu as a structural component makes these $[\text{}^{64}\text{Cu}]\text{CuS}$ NPs suited for multifunctional molecular imaging and therapy.

6. View to the future

Looking into the future of the field of nuclear molecular imaging, we have to think about the development of the next generation of radiopharmaceuticals combining variety of properties and allowing for the simultaneous performance of multiple functions. The great diversity of nanoparticle cores and biomolecules that can be attached to the nanoparticle surface, offers the possibility of creating multifunctional devices to be used in hybrid imaging platforms.

In the field of molecular therapy, some nanoparticles offer novel proposals for the delivery of therapeutic and target-specific drugs. Multifunctional radiolabeled nanoparticles can combine imaging and therapeutic agents in one preparation and specifically target the site of the disease (accumulate there) via both non-specific and specific mechanisms, such as the enhanced permeability and retention (EPR) effect for macromolecules (Maeda et al., 2000) and the ligand-mediated recognition.

In all clinically relevant imaging modalities, contrast agents are used to absorb certain types of signal much stronger than do the surrounding tissues. To still further increase a local spatial concentration of a contrast agent for better imaging, it is a natural progression to use

nanoparticles to carry multiple contrast moieties for an efficient enhancing of the signal from these areas (Torchilin, 2006).

A nanoparticle that has intrinsic imaging and therapeutic properties is advantageous. For gold and SWNT nanoparticles, the composition itself produces imaging contrast (optical imaging). Moreover, these nanoparticles have thermoablative properties. Local application of heat is a known concept in therapeutic medicine that has been extensively explored for cancer treatment and other conditions. Excitation sources, such as infrared lamps, ultrasound or lasers, can be used in the process, but there is always the problem of limiting the heat generated to just the area of the target tissue. This problem could be solved by using nanoparticles designed to absorb in the NIR region so that the resulting localized heating causes irreversible thermal cellular destruction. A laser irradiation (NIR light) of SWNT or gold nanoparticles leads to a rise in the temperature of the target regions from 40°C to 50°C, which selectively could destroy a carcinoma (Pissuwan et al., 2006).

An important benefit of receptor-specific radiopharmaceuticals is their use for targeted radiotherapy. Multiple specific biomolecules to target breast cancer cells, appended to one gold nanoparticle and labeled with an imaging radionuclide such as ^{99m}Tc as well as a β -particle-emitting radionuclide such as ^{90}Y , ^{177}Lu or ^{188}Re , could be a multifunctional system useful for the identification of malignant tumors (SPECT/NIR fluorescence imaging) and metastatic sites (avoiding immunohistochemistry studies), for targeted radiotherapy (high β -particle-energy delivered per unit of targeted mass) and for photothermal therapy (localized heating). Furthermore, ^{99m}Tc internalized in cancer cell nuclei acts as an effective system of targeted radiotherapy because of the Auger and internal conversion electron emissions near DNA. ^{99m}Tc -labeled gold nanoparticles described above and also conjugated to the HIV Tat(49-57) peptide to reach DNA, could potentially be a radiotherapeutic system at cellular level. However, for therapeutic purposes NPs should be administered by intratumoral injection or into a selective artery to avoid a high uptake by organs of the reticuloendothelial system because of the NPs' colloidal nature.

The traditional concept of separating diagnosis and treatment could conclude. The use of multifunctional radiolabeled nanoparticles that can simultaneously detect, image, and treat diseases may one day become the first alternative instead of the exception.

7. Conclusions

In our research we have demonstrated that it is possible to prepare stable hybrid radiolabeled gold nanoparticles. Multimeric systems of ^{99m}Tc -labeled gold nanoparticles conjugated to peptides or mannose can be prepared from kit formulations with high radiochemical purities (>94%). ^{99m}Tc -AuNP-Lys³-bombesin, ^{99m}Tc -AuNP-c[RDGfK(C)] and ^{99m}Tc -AuNP-mannose show properties suitable for use as target-specific agents for molecular imaging of GRP receptor-positive tumors, tumor $\alpha_v\beta_3$ expression and sentinel lymph node detection, respectively, with the possibility to be used as photothermal therapeutic systems.

Multifunctional nanoparticles can combine diagnostic and therapeutic capabilities for targeted-specific diagnosis and the treatment of disease. Medical imaging modalities such as SPECT, PET and MRI can identify tumors non-invasively, but radiolabeled nanoparticle

probes with multivalent properties can provide multimodal images with enhanced signal and sensitivity. Developments of radioactive QD-, AuNP-, SWNT-, CuS- or IO-target-specific biomolecules can be further developed to provide a visual guide during surgery. Radiolabeled SWNT and gold nanoparticles have a variety of real or potential applications in medical diagnosis and therapeutic treatments, due to their particularly combination of optical and photothermal properties. However, the work in this field is still in its infancy, and the achievement of more *in vivo* preclinical and clinical trials is required.

8. Acknowledgment

The authors are grateful for the support of the Mexican National Council of Science and Technology (CONACYT-SEP-CB-2010-01-150942).

9. References

- ASTM E 2456-06: *Standard Terminology related to Nanotechnology*. ASTM International, 100 Barr Harbor Drive, PO Box C700, West Conshohocken, PA, 19428-2959 USA (2006). <http://www.astm.org/Standards/E2456.htm>
- Berry, C.C.; de la Fuente, J.M.; Mullin, M.; Chu, S.W. & Curtis A.S. (2007). Nuclear Localization of HIV-1 Tat Functionalized Gold Nanoparticles. *IEEE Trans Nanobioscience*, Vol.6, No.4, (December 2007), pp. 262-269, ISSN 1536-1241
- Cai, W.; Chen, K.; Li, Z.B.; Gambhir, S.S. & Chen, X. (2007). Dual-Function Probe for PET and Near-Infrared Fluorescence Imaging of Tumor Vasculature. *Journal of Nuclear Medicine*, Vol.48, No.11, (November 2007), pp. 1862-1870, ISSN 0161-5505
- Cao, J.; Wang, Y.; Yu J.; Xia J.; Zhang C.; Yin D. & Häfeli U.O. (2004). Preparation and Radiolabeling of Surface-Modified Magnetic Nanoparticles with Rhenium-188 for Magnetic Targeted Radiotherapy. *Journal of Magnetism and Magnetic Materials*, Vol.277, No.1-2, (February 2004), pp. 165-174, ISSN 0304-8853
- Chan, H.B.S.; Ellis, B.L.; Sharma, H.L.; Frost, W.; Caps, V.; Shields, R.A. & Tsang, S.C. (2004). Carbon-Encapsulated Radioactive ^{99m}Tc Nanoparticles. *Advanced Materials*, Vol.16, No.2, (January 2004), pp. 144-149, ISSN 0935-9648
- Chen, K. & Conti, P.S. (2010). Target-Specific Delivery of Peptide-Based Probes for PET Imaging. *Advanced Drug Delivery Reviews*, Vol.62, No.11, (August 2010), pp. 1005-1022, ISSN 0169-409X
- Chen, K.; Li, Z-B.; Wang, H.; Cai, W. & Chen, X. (2010). Dual-modality Optical and Positron Emission Tomography Imaging of Vascular Endothelial Growth Factor Receptor on Tumor Vasculature Using Quantum Dots. *European Journal of Nuclear Medicine and Molecular Imaging*, Vol.35, No.12, (December 2010), pp. 2235-2244, ISSN 1619-7089
- Cheung, W.H.; Chan, V.S.; Pang, H.W.; Wong, M.K.; Guo, Z.H.; Tam, P.K.; Che, C.M.; Lin, C.L.; & Yu, W.Y. (2009). Conjugation of Latent Membrane Protein (LMP)-2 Epitope to Gold Nanoparticles as Highly Immunogenic Multiple Antigenic Peptides for Induction of Epstein-Barr Virus-Specific Cytotoxic T-lymphocyte Responses in Vitro. *Bioconjugate Chemistry*, Vol.20, No.1, (January 2009), pp. 24-31, ISSN 1520-4812

- Chrastina, A. & Schnitzer, J.E. (2010). Iodine-125 Radiolabeling of Silver Nanoparticles for in Vivo SPECT Imaging. *International Journal of Nanomedicine*, Vol.5, (September 2010), pp. 653-659, ISSN 1176-9114
- Connor, E.E.; Mwamuka, J.; Gole, A.; Murphy, C.J. & Wyatt, M.D. (2005). Gold Nanoparticles Are Taken Up by Human Cells But Do Not Cause Acute Cytotoxicity. *Small*, Vol.1, No.3, (March, 2005), pp. 325-327, ISSN 1613-6810
- Daniel, M.C. & Astruc, D. (2004). Gold Nanoparticles: Assembly, Supramolecular Chemistry, Quantum-Size-Related Properties, and Applications Toward Biology, Catalysis, and Nanotechnology. *Chemical Reviews*, Vol.104, No.1, (January 2004), pp. 293-346, ISSN 0009-2665
- Devaraj, N.K.; Keliher, E.J.; Thurber, G.M.; Nahrendorf, M. & Weissleder, R. (2009). ¹⁸F-Labeled Nanoparticles for In Vivo PET/CT Imaging. *Bioconjugate Chemistry*, Vol.20, No.2, pp. 397-401, (February 2009), ISSN 1520-4812
- Dumortier, H.; Lacotte, S.; Pastorin, G.; Marega, R.; Wu, W.; Bonifazi, D.; Briand, J.P.; Prato, M.; Muller, S. & Bianco, A. (2006). Functionalized Carbon Nanotubes are Non-Cytotoxic and Preserve the Functionality of Primary Immune Cells. *Nano Letters*, Vol.6, No.7, (July 2006), pp. 1522-1528, ISSN 1530-6984
- Erathodiyil N. & Ying J.Y. (2011). Functionalization of Inorganic Nanoparticles for Bioimaging Applications. *Accounts of Chemical Research*, DOI: 10.1021/ar2000327, (June 2011), ISSN 1968-12010
- Ferro-Flores, G.; Arteaga de Murphy, C.; Rodriguez-Cortes, J.; Pedraza-Lopez, M. & Ramirez-Iglesias, M.T. (2006). Preparation and Evaluation of ^{99m}Tc-EDDA/HYNIC-[Lys³]-bombesin for Imaging of GRP Receptor-Positive Tumours. *Nuclear Medicine Communications*, Vol.27, No.4, (April 2006), pp. 371-376, ISSN 0143-3636
- Ferro-Flores, G.; Ramirez, F. de M.; Melendez-Alafort, L. & Santos-Cuevas, C.L. (2010a). Peptides for In Vivo Target-Specific Cancer Imaging. *Mini Reviews in Medicinal Chemistry*, Vol.10, No.1, (January, 2010), pp. 87-97, ISSN 1389-5575
- Ferro-Flores, G.; Ocampo-Garcia B.E.; Ramirez F. de M.; Gutierrez-Wing C.; Arteaga de Murphy C. & Santos-Cuevas C.L. (2010b). Gold Nanoparticles Conjugated to Peptides, In: *Colloids in Biotechnology*, M. Fanun, (Ed.), 231-252, CRC Press/Taylor & Francis, ISBN: 978-143-983-080-2, Boca Raton, FL, United States of America
- Gao, X.H.; Cui, Y.Y.; Levenson, R.M.; Chung, L.W.K.; Nie, S.M. (2004). In Vivo Cancer Targeting and Imaging with Semiconductor Quantum Dots. *Nature Biotechnology*, Vol.22, No.8, (August 2004), pp.969-966, ISSN 1087-0156
- Giljohann, D.A.; Seferos, D.S.; Daniel, W.L.; Massich, M.D.; Patel, P.C. & Mirkin, C. A. (2010). Gold Nanoparticles for Biology and Medicine. *Angewandte Chemie International Edition*, Vol.49, No.19, (April 2010), pp.3280-3294, ISSN 0570-0833
- Glaus, C.; Rossin, R.; Welch, M.J. & Bao, G. (2010). In Vivo Evaluation of ⁶⁴Cu-Labeled Magnetic Nanoparticles as a Dual-Modality PET/MR Imaging Agent. *Bioconjugate Chemistry*, Vol. 21, No.4, (April 2010), pp. 715-722, ISSN 1043-1802
- Guo, J.; Zhang, X.; Li, Q. & Li, W. (2007). Biodistribution of Functionalized Multiwall Carbon Nanotubes in mice. *Nuclear Medicine and Biology*, Vol.34, No.5, (May 2007), pp. 579-583, ISSN 0969-8051

- Hata, K.; Futaba, D.N.; Mizuno, K.; Namai, T.; Yumura M. & Iijima S. (2004). Water-Assisted Highly Efficient Synthesis of Impurity-Free Single-Walled Carbon Nanotubes. *Science*, Vol.306, No.5700, (November 2004), pp.1362-1364, ISSN 0036-8075
- Hong, H.; Zhang, Y.; Sun, J. & Cai, W. (2009a). Molecular Imaging and Therapy of Cancer with Radiolabeled Nanoparticles. *Nanotoday*, Vol.4., No.5, (October 2009), pp. 399-413, ISSN 1748-0132
- Hong, H.; Gao, T. & Cai, W. (2009b). Molecular Imaging with Single-Walled Carbon Nanotubes. *Nanotoday*, Vol.4, No.3, (July 2009), pp.252-261, ISSN 1748-0132
- Huang, X.; Neretina, S. & El-Sayed, M.A. (2009). Gold Nanorods: From Synthesis and Properties to Biological and Biomedical Applications. *Advanced Materials*, Vol.21, No.48, (December 2009), pp. 4880–4910, ISSN 0935-9648
- Hwang, D.W.; Ko, H.Y.; Kim, S.K.; Kim, D.; Lee, D.S. & Kim, S. (2009). Development of a Quadruple Imaging Modality by Using Nanoparticles. *Chemistry- A European Journal*, Vol.15, No.37, (September 2009), pp. 9387-9393, ISSN 1521-3765
- Jadzinsky, P.D.; Calero, G.; Ackerson, C.J.; Bushnell, D.A. & Komberg, R.D. (2007). Structure of a Thiol Monolayer-Protected Gold Nanoparticle at 1.1 Å Resolution. *Science*, Vol.318, No.5849, (September 2007), pp. 430-433, ISSN 0036-8075
- Jarrett, B.R.; Gustafsson, B.; Kukis, D.L. & Louie, A.Y. (2008). Synthesis of ⁶⁴Cu-Labeled Magnetic Nanoparticles for Multimodal Imaging. *Bioconjugate Chemistry*, Vol.19, No.7, (July 2008), pp.1496–1504, ISSN 1043-1802
- Kam, N.W.S.; O'Connell, M.; Wisdom, J.A. & Dai, H. (2005). Carbon Nanotubes as Multifunctional Biological Transporters and Near-infrared Agents for Selective Cancer Cell Destruction. *Proceedings of the National Academy of Sciences of the United States of America*, Vol.102, No.33, (August 2005), pp.11600–11605, ISSN 0027-8424
- Kogan, M.J.; Olmedo, I.; Hosta, L.; Guerrero, A R.; Cruz L.J. & Albericio F. (2007). Peptides and Metallic Nanoparticles for Biomedical Applications. *Nanomedicine*, Vol.2, No.3, (June 2007), pp.287-306, ISSN 1743-5889
- Kubas, H.; Schafer, M.; Bauder-Wust, U.; Eder, M.; Oltmanns, D.; Haberkorn, U.; Mier, W. & Eisenhut, M. (2010). Multivalent Cyclic RGD Ligands: Influence of Linker Lengths on Receptor Binding. *Nuclear Medicine and Biology*, Vol.37, No.8, (November 2010), pp. 885–891. ISSN 0969-8051
- Kucka, J.; Hruby, M.; Konak, C.; Kozempel, J. & Lebeda, O. (2006). Astatination of Nanoparticles Containing Silver as Possible Carriers of ²¹¹At. *Applied Radiation and Isotopes*, Vol.64, No. 2, (February 2006), pp. 201-206, ISSN 1872-9800
- Lee, H.Y.; Li, Z.; Chen, K.; Hsu, A.R.; Xu, C.; Xie, J.; Sun, S. & Chen, X. (2008). PET/MRI Dual-Modality Tumor Imaging Using Arginine-Glycine-Aspartic (RGD)-Conjugated Radiolabeled Iron Oxide Nanoparticles. *Journal of Nuclear Medicine*, Vol.49, No.8, (April 2008), pp. 1371–1379, ISSN 0161-5505
- Levy, R.; Thanh, N.T.K.; Doty, R.C.; Hussain, I.; Nichols, R.J.; Schiffrin, D.J.; Brust M. & Ferning, D.G., (2004). Rational and Combinatorial Design of Peptide Capping Ligands for Gold Nanoparticles. *Journal of American Chemical Society*, Vol.126, No.32, (July 2004), pp. 10076-10084, ISSN 0002-7863

- Liang, S.; Wang, Y.; Yu, J.; Zhang, C.; Xia, J. & Yin, D. (2007). Surface Modified Superparamagnetic Iron Oxide Nanoparticles: As a New Carrier for Bio-Magnetically Targeted Therapy. *Journal of Materials Science: Materials in Medicine*, Vol.18, No.12, (December 2007), pp. 2297-2302, ISSN 0957-4530
- Liu, S. (2008). Bifunctional Coupling Agents for Radiolabeling of Biomolecules and Target-specific Delivery of Metallic Radionuclides. *Advanced Drug Delivery Reviews*, Vol.60, No.12, (September 2008), pp. 1347-1370, ISSN 0169-409x
- Liu, S. (2009). Radiolabeled cyclic RGD Peptides as Integrin $\alpha_v\beta_3$ -Targeted Radiotracers: Maximizing Binding Affinity Via Bivalency. *Bioconjugate Chemistry*, Vol.20, No.12, (December 2009), pp.2199-2213, ISSN 1520-4812
- Liu, Z.; Cai, W.; He, L.; Nakayama, N.; Chen, K.; Sun, X.; Chen, X. & Dai, H. (2007). In vivo Biodistribution and Highly Efficient Tumor Targeting of Carbon Nanotubes in Mice. *Nature Nanotechnology*, Vol.2, No.1, (January 2007), pp.47-52, ISSN 1748-3395
- Madsen, M.T. (2007). Recent Advances in SPECT Imaging. *Journal of Nuclear Medicine*, Vol.48, No.4, (April 2007), pp. 661-673, ISSN 0161-5505
- Maeda, H.; Wu, J.; Sawa, T.; Matsumura, Y. & Hori, K. (2000). Tumor vascular permeability and the EPR effect in macromolecular therapeutics: a review. *Journal of Controlled Release*, Vol.65, No.1-2, (March 2000), pp. 271-284, ISSN 0168-3659
- Massoud, T.F. & Gamghir, S.S. (2003). Molecular Imaging in Living Subjects: Seeing Fundamental Biological Processes in a New Light. *Genes and Development*, Vol.17, No.5, (May 2003), pp. 545-580, ISSN 0890-9369
- McDevitt, M.R.; Chattopadhyay, D.; Kappel, B.J.; Jaggi, J.S.; Schiffman, S.R.; Antczak, C.; Njardarson, J.T.; Brentjens, R. & Scheinberg D.A. (2007). Tumor Targeting with Antibody-Functionalized Radiolabeled Carbon Nanotubes. *Journal of Nuclear Medicine*, Vol.48, No.7, (July 2007), pp. 1180-1189, ISSN 0161-5505
- Mendoza-Sanchez, A.N.; Ferro-Flores, G.; Ocampo-Garcia, B.E.; Morales-Avila, E.; Ramirez, F. de M.; De Leon-Rodriguez, L.M.; Santos-Cuevas, C.L.; Medina, L.A.; Rojas-Calderon, E.L. & Camacho-Lopez M.A. (2010). Lys³-Bombesin Conjugated to ^{99m}Tc-Labelled Gold Nanoparticles for In Vivo Gastrin Releasing Peptide-Receptor Imaging. *Journal of Biomedical Nanotechnology*, Vol.6, No.4 (August 2010), pp. 375-384, ISSN 1550-7033
- Montet, X.; Funovics, M.; Montet-Abou, K.; Weissleder, R. & Josephson, L. (2006). Multivalent Effects of RGD Peptides Obtained by Nanoparticle Display. *Journal of Medicinal Chemistry*, Vol.49, No.20, (September 2006), pp. 6087-6093, ISSN 0022-2623
- Morales-Avila, E.; Ferro-Flores, G.; Ocampo-Garcia, B.E.; De Leon, L.M.; Santos-Cuevas, C.L.; Medina, L.A. & Gomez-Olivan L. (2011). Multimeric System of ^{99m}Tc-labeled Gold Nanoparticles Conjugated to c[RGDfK(C)] for Molecular Imaging of Tumour $\alpha_v\beta_3$ expression. *Bioconjugate Chemistry*, Vol.22, No.5, (May 2011), pp. 913-922, ISSN 1043-1802
- Ocampo-Garcia, B.E.; Ferro-Flores, G.; Morales-Avila, E. & Ramirez, F. de M. (2011a). Kit for Preparation of Multimeric Receptor-Specific ^{99m}Tc-Radiopharmaceuticals Based on Gold Nanoparticles. *Nuclear Medicine Communications*, Vol. 32, No.11 (November 2011), pp. 1095-1104, ISSN 0143-3636

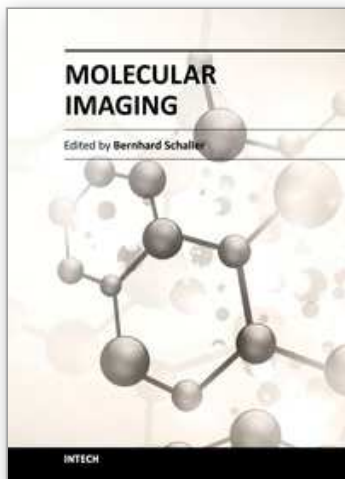
- Ocampo-Garcia, B.E.; Ramirez, F. de M.; Ferro-Flores, G.; Leon-Rodriguez, L.M.; Santos-Cuevas, C.L.; Morales-Avila, E.; Arteaga de Murphy, C.; Pedraza-Lopez, M.; Medina, L.A. & Camacho-Lopez, M.A. (2011b). ^{99m}Tc -labeled Gold Nanoparticles Capped with HYNIC Peptide/Mannose for Sentinel Lymph Node Detection. *Nuclear Medicine and Biology*, Vol.38, No.1, (January 2011), pp. 1-11, ISSN 0969-8051
- Pissuwan, D.; Valenzuela, S.M. & Cortie, M.B. Therapeutic possibilities of plasmonically heated gold nanoparticles. *Trends in Biotechnology*, Vol.24, No.2, (February 2006), pp. 62-67, ISSN 0167-7799
- Porta, F.; Speranza, G.; Krpetic, Z.; Santo, V.D.; Francescato, P. & Scari, G. (2007). Gold Nanoparticles Capped by Peptides. *Materials Science and Engineering: B*, Vol.140, No.3 (June 2007), pp. 187-194, ISSN 0921-5107
- Qingnuan, L.; Yan, X.; Xiaodong, Z.; Ruili, L.; Qieqie, D.; Xiaoguang, S.; Shaoliang, C. & Wenxin, L. (2002). Preparation of ^{99m}Tc - $\text{C}_{60}(\text{OH})_x$ and its Biodistribution Studies. *Nuclear Medicine and Biology*, Vol.29, No.6, (June 2002), pp. 707-710, ISSN 0969-8051
- Santos-Cuevas, C.L.; Ferro-Flores, G.; Arteaga de Murphy, C. & Pichardo-Romero, P. (2008) Targeted Imaging of GRP Receptors with ^{99m}Tc -EDDA/HYNIC-[Lys³]-Bombesin: Biokinetics and Dosimetry in Women. *Nuclear Medicine Communications*, Vol.29, No.8, (August 2008), pp. 741-747, ISSN 0143-3636
- Santos-Cuevas, C.L.; Ferro-Flores, G.; Rojas-Calderon, E.L.; Garcia-Becerra, R.; Ordaz-Rosado, D.; Arteaga de Murphy, C. & Pedraza-Lopez, M. (2011). ^{99m}Tc - N_2S_2 -Tat(49-57)-Bombesin Internalized in Nuclei of Prostate and Breast Cancer Cells: Kinetics, Dosimetry and Effect on Cellular Proliferation. *Nuclear Medicine Communications*, Vol.32, No.4, (April 2011), pp. 303-313, ISSN 0143-3636
- Singh, R.; Pantarotto, D.; Lacerda, L.; Pastorin, G.; Klumpp, C.; Prato, M.; Bianco, A.; Kostarelos, K. (2006). Tissue Biodistribution and Blood Clearance Rates of Intravenously Administered Carbon Nanotube Radiotracers. *Proceedings of the National Academy of Sciences of the United States of America*, Vol.103, No.9, (February 2006), pp. 3357-62, ISSN 0027-8424
- Stelter, L.; Pinkernelle, J.G.; Michel, R.; Schwartlander, R.; Raschzok, N.; Morgul, M.H.; Koch, M.; Denecke, T.; Ruf, J. & Baumler, H. (2009). Modification of Aminosilanized Superparamagnetic Nanoparticles: Feasibility of Multimodal Detection Using 3T MRI, Small Animal PET, and Fluorescence Imaging. *Molecular Imaging and Biology*, Vol.12, No.1, (January 2009), pp. 25-34, ISSN 1536-1632
- Sun, Y. & Xia, Y. (2002). Shape-Controlled Synthesis of Gold and Silver Nanoparticles. *Science*, Vol. 298, No.5601, (December, 2002), pp. 2176-2179, ISSN 0036-8075
- Surujpaul, P.P.; Gutierrez-Wing, C.; Ocampo-Garcia, B.E.; Ramirez, F. de M.; Arteaga de Murphy, C.; Pedraza-Lopez, M.; Camacho-Lopez, M.A. & Ferro-Flores, G. (2008). Gold nanoparticles conjugated to [Tyr³]octreotide peptide. *Biophysical Chemistry*, Vol.138, No.3, (December 2008), pp. 83-90, ISSN 0301-4622
- Takagi, K.; Uehara, T.; Kaneko, E.; Nakayama, M.; Koizumi, M.; Endo, E. & Arano, Y. (2004). ^{99m}Tc -labeled Mannosyl-Neoglycoalbumin for Sentinel Lymph Node Identification.

- Nuclear Medicine and Biology*, Vol.31, No.7, (October 2003), pp. 893-900, ISSN 0969-8051
- Torchilin, V.P. (2006). Multifunctional nanocarriers. *Advanced Drug Delivery Reviews*, Vol.58, No.14, (December 2006), pp. 1532-1555, ISSN 0169-409X
- Torres Martin de Rosales, R.; Tavare, R.; Glaria, A.; Varma, G.; Protti, A. & Blower P.J. (2011). ^{99m}Tc-Bisphosphonate-Iron Oxide Nanoparticle Conjugates for Dual-Modality Biomedical Imaging. *Bioconjugate Chemistry*, Vol.22, No.3, (March 2010), pp. 455-465, ISSN 1043-1802
- Vera, D.R.; Wallace, A.M.; Hoh, C.K. & Mattrey, R.F. (2001). A Synthetic Macromolecule for Sentinel Node Detection: ^{99m}Tc-DTPA-Mannosyl-dextran. *Journal of Nuclear Medicine*, Vol.42, No.6, (June 2001), pp. 951-959, ISSN 0161-5505
- Wang, Z.; Levy, R.; Fernig, D.G. & Brust, M. (2005). The Peptide Route to Multifunctional Gold Nanoparticles. *Bioconjugate Chemistry*, Vol.16, No.3, (April 2005), pp. 497-500, ISSN 1043-1802
- Xie, H.; Diagaradjane, P.; Deorukhkar, A.A.; Goins, B.; Bao, A.; Phillips, W.T.; Wang, Z.; Schwartz, J. & Krishnan, S. (2011). Integrin $\alpha_v\beta_3$ -Targeted Gold Nanoshells Augment Tumor Vasculature-Specific Imaging and Therapy. *International Journal of Nanomedicine*, Vol. 6, (January 27), pp. 259-269, ISSN 1178-2013
- Xie, J.; Chen, K.; Huang, J.; Lee, S.; Wang, J.; Gao, J. & Li, X. (2010). PET/NIRF/MRI Triple Functional Iron Oxide Nanoparticles. *Biomaterials*, Vol.31, No.11, (April 2010) pp.3016-3022, ISSN 0142-9612
- Xie, R.; Chen, K.; Chen, X. & Peng, X. (2008). InAs/InP/ZnSe Core/Shell/Shell Quantum Dots as Near-Infrared Emitters: Bright, Narrow-Band, Non-Cadmium Containing, and Biocompatible. *Nano Research*, Vol.1, No 6, (October 2008), pp. 457-464, ISSN 1931-7573
- Yang, X.; Hong, H.; Grailer, J.J.; Rowland, I. J.; Javadi A.; Hurley, S.A.; Xiao, Y.; Yang, Y.; Zhang, Y.; Nickles, R. J.; Cai, W. & Steeber, D.A. (2011). cRGD-Functionalized, DOX-Conjugated, and ⁶⁴Cu-labeled Superparamagnetic Iron Oxide Nanoparticles for Targeted Anticancer Drug Delivery and PET/MR Imaging. *Biomaterials*, Vol.32, No. 17, (June 2011), pp. 4151-4160, ISSN 0142-9612.
- Yu, W.W.; Wang, Y.A. & Peng, X.G. (2003). Formation and Stability of Size-, Shape-, and Structure-Controlled CdTe Nanocrystals: Ligand Effects on Monomers and Nanocrystals. *Chemistry of Materials*, Vol.15, No.22, (October 2003), pp. 4300-4308, ISSN 1520-5002
- Zhang, L.X.; Sun, X.P.; Song, Y.H.; Jiang, X.; Dong, S.J. & Wang, E.A. (2006). Didodecyldimethylammonium Bromide Lipid Bilayer-Protected Gold Nanoparticles: Synthesis, Characterization, and Self-Assembly. *Langmuir*, Vol.22, No.6, (March, 2006), pp. 2838-2843, ISSN 1520-5827
- Zhang, G.; Yang, Z.; Lu, W.; Zhang, R.; Huang, Q.; Tian, M.; Li, L.; Liang, D. & Li, C. (2009). Influence of Anchoring Ligands and Particle Size on the Colloidal Stability and *in vivo* Biodistribution of Polyethylene Glycol-Coated Gold Nanoparticles in Tumor-Xenografted Mice. *Biomaterials*, Vol.30, No.10, (April 2009), pp. 1928-1936, ISSN 1878-5905.

Zhou, M.; Zhang, R.; Huang, M.; Lu, W.; Song, S.; Melancon, M.P.; Tian, M.; Liang, D. & Li, C. (2010). A Chelator-Free Multifunctional [^{64}Cu]CuS Nanoparticle Platform for Simultaneous Micro-PET/CT Imaging and Photothermal Ablation Therapy. *Journal of American Chemical Society*, Vol.132, No.43, (October 2010), pp.15351-15358, ISSN 0002-7863

IntechOpen

IntechOpen



Molecular Imaging

Edited by Prof. Bernhard Schaller

ISBN 978-953-51-0359-2

Hard cover, 390 pages

Publisher InTech

Published online 16, March, 2012

Published in print edition March, 2012

The present book gives an exceptional overview of molecular imaging. Practical approach represents the red thread through the whole book, covering at the same time detailed background information that goes very deep into molecular as well as cellular level. Ideas how molecular imaging will develop in the near future present a special delicacy. This should be of special interest as the contributors are members of leading research groups from all over the world.

How to reference

In order to correctly reference this scholarly work, feel free to copy and paste the following:

Enrique Morales-Avila, Guillermina Ferro-Flores, Blanca E. Ocampo-García and Flor de María Ramírez (2012). Radiolabeled Nanoparticles for Molecular Imaging, Molecular Imaging, Prof. Bernhard Schaller (Ed.), ISBN: 978-953-51-0359-2, InTech, Available from: <http://www.intechopen.com/books/molecular-imaging/radiolabeled-nanoparticles-for-molecular-imaging>

INTECH
open science | open minds

InTech Europe

University Campus STeP Ri
Slavka Krautzeka 83/A
51000 Rijeka, Croatia
Phone: +385 (51) 770 447
Fax: +385 (51) 686 166
www.intechopen.com

InTech China

Unit 405, Office Block, Hotel Equatorial Shanghai
No.65, Yan An Road (West), Shanghai, 200040, China
中国上海市延安西路65号上海国际贵都大饭店办公楼405单元
Phone: +86-21-62489820
Fax: +86-21-62489821

© 2012 The Author(s). Licensee IntechOpen. This is an open access article distributed under the terms of the [Creative Commons Attribution 3.0 License](#), which permits unrestricted use, distribution, and reproduction in any medium, provided the original work is properly cited.

IntechOpen

IntechOpen